A PREDICTION METHOD OF NON-STRUCTURAL RESPONSE SPECTRA
Part 1: Outline of Prediction Method and Verification with SDOF Building

K. Kasai[1], S. Komatsu[2], and D. Lau[3]

[1] *Specially Appointed Professor, Tokyo Institute of Technology, kasai.k.ac@m.titech.ac.jp*
[2] *Assistant Professor, Shimane University, s.komatsu@riko.shimane-u.ac.jp*
[3] *Professor, Carleton University, DavidLau@cunet.carleton.ca*

Abstract

The 2011 Great East Japan earthquake caused significant damages to non-structural components and substantial economic losses. Because of such adverse effects, seismic response evaluation for various components is becoming increasingly important. The response of non-structural component can be evaluated through time history response analysis by modeling the components as secondary systems attached to the building. However, the time history analysis approach is time-consuming and does not lend itself readily to design applications. For design purposes, a simplified prediction method to give accurate response spectra of non-structural components is very helpful. Previously developed methods sometimes have inconsistent accuracy because of limitations on the parameters used. Also, most of the previous studies focus on only acceleration responses, while displacement responses are also considered important in recent years. This paper proposes a simplified method to obtain spectral displacement and spectral pseudo-acceleration of non-structural components in buildings. In Part 1, the prediction method for the response spectra of non-structural components attached to the *j*-th mode SDOF building model and the accuracy of the prediction are described. The companion paper (Part 2) discusses combinations of such spectral values.

Keywords: non-structural components; response prediction; response spectra; duration of ground motions

1. Introduction

After the 2011 Great East Japan earthquake, damage to non-structural components such as suspended ceiling and equipment attracts the interest of structural engineers. Extensive damage of the non-structural components due to their high acceleration and/or large displacement responses led to substantial economic losses of many companies [1]. Therefore, it is clear that in order to improve safety of the residential space and sustainability of the equipment, there is an urgent need for developing better prediction models for the non-structural components in buildings during earthquakes.

Floor response spectra calculated by considering the non-structural components as a single-degree-of-freedom (SDOF) system are widely used for current response evaluation. In contrast to this, the methods that directly generate floor response spectra from given seismic response spectra has been proposed by many researchers. The method establishes a mathematical relation between characteristics of the ground motion, dynamic properties of the building and non-structural components, and the non-structural maximum response. Thus it facilitates the understanding of the physical link from seismic input to the non-structural response via the building response, and simplification of the response evaluation.

In the new prediction method, the building response spectrum and duration of ground motion are taken into account as seismic input characteristics. Also, the influences of the building natural periods and damping ratios in multiple modes, and the natural period and damping ratio of the non-structural components are considered. There are some previouce studies on the generation method only for acceleration responses that did not consider the effects of all these significant characteristic parameters as pointed out here [1 to 8].

The objective of this paper is to present a direct method that can directly generate the non-structural response spectra from the building response spectrum with consideration of the characteristics of the input ground motion, building, and non-structural components. The method assumes the responses of the building and non-structural components remain in the elastic range, and it takes into account various spectral characteristics, the duration of the ground motions, and high-order modal responses of the building. Further, an expansion of the method to multi-story buildings is described in Part 2 [9].

2. Response characteristics of SDOF building and non-structural component models

2.1 Outline of building and non-structural component models

A multi-story building is represented by a multi-degree-of-freedom (MDOF) model as shown in Fig. 1a. To generate non-structural response spectra, it is essential to recognize that the contribution of each modal response is different at each story as shown in Fig. 1a. The *j*-th modal building natural period and damping ratio are $T_{bj} = 2\pi / \omega_{bj}$ and h_{bj}, respectively; and for non-structural component, the natural period and damping ratio are $T_c = 2\pi / \omega_c$ and h_c, respectively. The building's and components' equations of motion are expressed as Equation (1a, b), where they are modeled by SDOF models as shown in Fig. 1b.
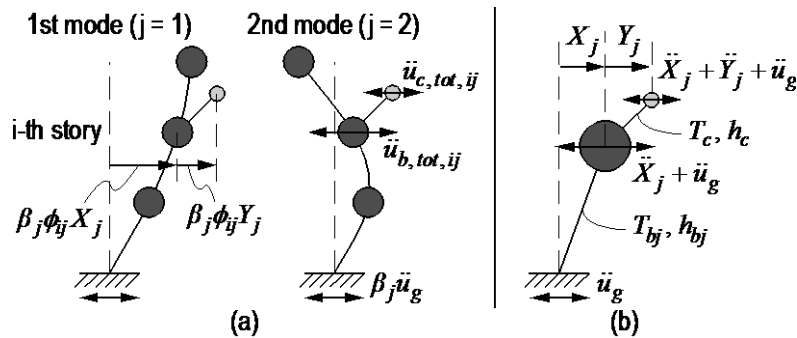

Fig. 1 – Relationship between MDOF model and SDOF model

$$\ddot{X}_j(t) + 2h_{bj}\omega_{bj}\dot{X}_j(t) + \omega_{bj}{}^2 X_j(t) = -\ddot{u}_g(t)$$

$$\ddot{Y}_j(t) + 2h_c\omega_c\dot{Y}_j(t) + \omega_c{}^2 Y_j(t) = -(\ddot{X}_j(t) + \ddot{u}_g(t))$$

(1a, b)

where $\ddot{u}_g(t)$ = ground acceleration of input seismic wave, $X_j(t)$ = relative displacement of the SDOF building model with the *j*-th mode building natural period and damping ratio, and $Y_j(t)$ = relative displacement of the non-structural component against the SDOF building model. By using these solutions $\ddot{X}_j(t)$, $\ddot{Y}_j(t)$, the *j*-th mode contributions to the building and component (Fig. 1a) are obtained by Equation (2) as follows

$$\ddot{u}_{b,tot,ij}(t) = \beta_j\phi_{ij}(\ddot{X}_j(t) + \ddot{u}_g(t))$$

$$\ddot{u}_{c,tot,ij}(t) = \beta_j\phi_{ij}(\ddot{X}_j(t) + \ddot{Y}_j(t) + \ddot{u}_g(t))$$

(2a, b)

where $\ddot{u}_{b,tot,ij}(t)$ = the *i*-th story of the *j*-th modal building absolute acceleration response, $\ddot{u}_{c,tot,ij}(t)$ = absolute acceleration response of the non-structural components due to the excitation from the *j*-th modal response of the building at the *i*-th story, $\beta_j\phi_{ij}$ = the *i*-th story element of the *j*-th modal participation vector, β_j = the *j*-th modal participation factor. The participation factor and vector can be obtained by Equations (3a, b) as follows.

$$\beta_j = \sum_{i=1}^{N} m_i\phi_{ij} \Big/ \sum_{i=1}^{N} m_i\phi_{ij}{}^2, \qquad \sum_{j=1}^{N} \beta_j\phi_{ij} = 1$$

(3a, b)

2

where N = story of the building, m_i = mass of the i-th story.

Conversely, if only the maximum response is needed, a response spectrum method that gives comprehensive solutions for different combinations of T_c and h_c is useful. The method generates non-structural pseudo-acceleration spectra $S_{pac,j}(T_c, h_c)$ from building pseudo-acceleration spectra $S_{pa}(T_{bj}, h_{bj})$. From this and Equation (2), the response of the components at the i-th story subjected to the j-th modal building response are predicted as follows

$$|\ddot{u}_{b,tot,ij}(t)|_{\max} \approx |\beta_j \phi_{ij}| S_{pa}(T_{bj}, h_{bj})$$

$$|\ddot{u}_{c,tot,ij}(t)|_{\max} \approx |\beta_j \phi_{ij}| S_{pac,j}(T_c, h_c)$$

(4a, b)

The relation between pseudo-acceleration and displacement spectra is expressed by Equation (5) as follows

$$S_{pa}(T_{bj}, h_{bj}) = \omega_{bj}^2 S_d(T_{bj}, h_{bj})$$

$$S_{pac,j}(T_c, h_c) = \omega_c^2 S_{dc,j}(T_c, h_c)$$

(5a, b)

where $S_{dc,j}(T_c, h_c)$ is relative displacement of the components against the building floor. Moreover, even the maximum damping ratios h_{bj}, $h_c = 0.1$ considered in this paper, the difference between the maximum values of pure absolute acceleration and pseudo-acceleration was only about 2%.

2.2 Trend of building accelerations

This section examines the absolute acceleration response $\ddot{X}_j(t) + \ddot{u}_g(t)$ obtained by using the SDOF building model shown in Fig. 1b. Table 1 shows the 16 earthquake records used as input excitations and their duration of the ground motions t_d which is taken from Trifnac and Brady [10] as the time interval of the seismic energy released between 5 to 95% of the earthquake event.

Table 1 – List of input seismic waves

Earthquake		PGA (gal)	Input time (s)	Duration t_d (s)
Northridge (1994)	Newhall NS	578	60	5.5
	Newhall EW	572	60	5.9
	Sylmar NS	827	60	5.32
	Sylmar EW	593	60	7.06
Hyogoken nanbu (1995)	JMA Kobe NS	821	30	8.1
Iran (1978)	Tabas N344E	919	50	18.1
	Tabas N074E	863	50	18.4
Imperial valley (1940)	El Centro NS	342	54	24.4
Tokachi-oki (1968)	Hachinohe EW	180	51	24.8
Kern country (1952)	Taft EW	176	54	28.8
Chichi (1999)	TCU065 NS	563	160	28.9
	TCU065 EW	774	160	29.2
Kocaeli (1999)	Sakarya	407	389	44.3
Artificial	BCJ-L2	356	120	65.3
Tokachi-oki (2003)	Tomakomai EW	72.9	291	89.5
Tohoku (2011)	Kogakuin NS	88.5	300	113

For T_{bj} = 0.5, 2, 5s, h_{bj} = 0.02, 0.1, and Taft EW or Tomakomai EW, the response $\ddot{X}_j(t) + \ddot{u}_g(t)$ has a stationary trend in its behavior which is evidenced by several cycles having almost the same amplitude and

3

period T_{bj} around the maximum response as shown by the white circle in Fig. 2. This trend is observed in all cases of the 16 earthquake records, all three cases of the building natural period, and ten cases of the damping ratio 0.01 to 0.1 ($16 \times 3 \times 10 = 480$ cases). Therefore, this behavior in the response is assumed hereafter.
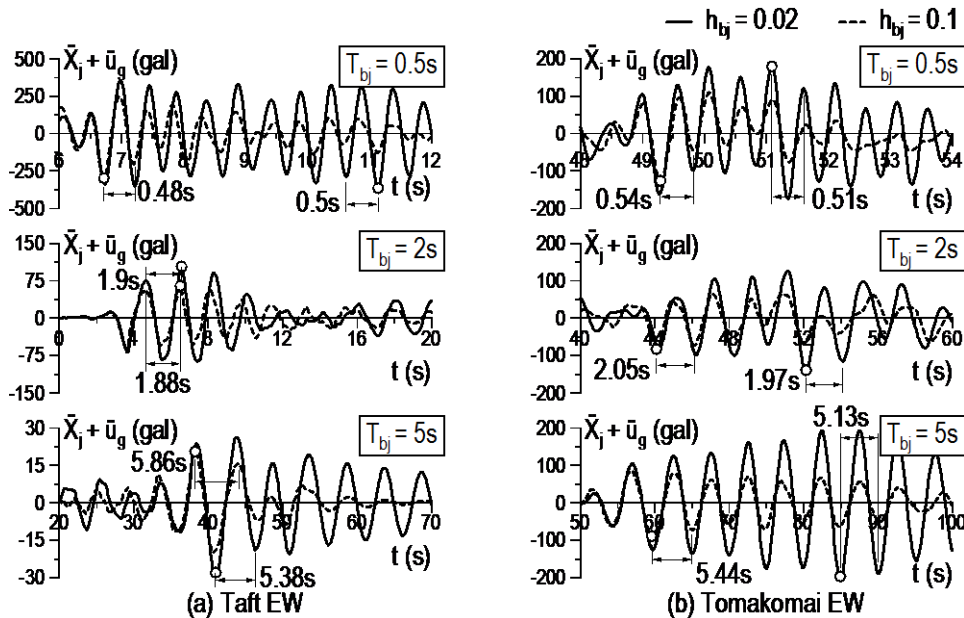

Fig. 2 – Abs. acc. response time histories of SDOF buildings (○ = maximum response)

2.3 Trend of non-structural accelerations

To investigate the response characteristics of the non-structural components $\ddot{X}_j(t) + \ddot{Y}_j(t) + \ddot{u}_g(t)$, the building response of the SDOF model with $T_{bj} = 2$s and $h_{bj} = 0.02$ is used as input excitation to the non-structural components with the varying properties of $T_c = 0.5, 2, 5$s and $h_c = 0.02, 0.1$.
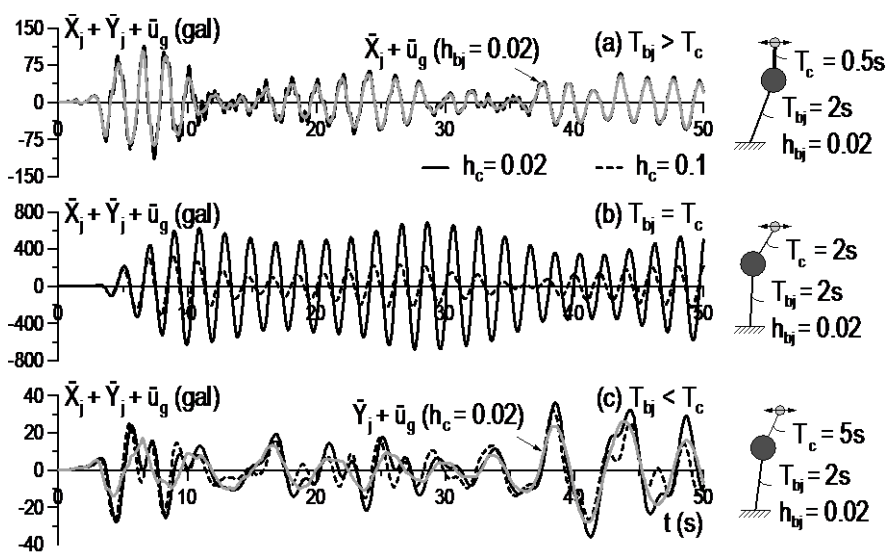

Fig. 3 – Left: Abs. acc. response time histories of components (Taft EW)
Right: maximum displacement ratio of X_j and Y_j for $h_c = 0.02$

4

For $T_c = 0.5$s $< T_{bj}$ in Fig. 3a, the response $X_j(t)$ is predominated, hence the building response as input to the non-structural component is controlled by the period component T_{bj}. This is evidenced by the non-structural responses (solid and dash lines) are almost the same as the building response $\ddot{X}_j(t) + \ddot{u}_g(t)$ (gray line). For $T_c = 2$s $= T_{bj}$ in Fig. 3b, the non-structural response is amplified due to resonance (solid line), and it is greatly affected by h_c (dash line). For $T_c = 5$s $> T_{bj}$ in Fig. 3c, the response $Y_j(t)$ is dominated by the non-structural response. It shows a tendency that the non-structural component response can be estimated by considering the component is directly excited by the seismic input in contrast to Fig. 3a. This result can be understood from the similarity of the non-structural response (the solid line) and the response $\ddot{Y}_j(t) + \ddot{u}_g(t)$ (gray line) when the seismic motion is directly input to the non-structural component with $h_c = 0.02$. On these premise, the formulation of two transfer functions is presented in the next section.

3. Response prediction of SDOF components attached to SDOF building

3.1 Prediction formula 1 which considered the tendency of stationary response

In the tendency of stationary response as mentioned in section 2.3, the input vibration to the components had the building period component T_{bj}, hence this prediction formula 1 assumes the harmonic acceleration input with the amplitude $S_{pa}(T_{bj}, h_{bj})$ and period T_{bj}. Prediction formula 1 for non-structural response spectra $S_{pac,j}(T_c, h_c)$ is expressed as follows

$$S_{pac,j}(T_c, h_c) = \left| H_c(T_c / T_{bj}, h_c) \right| S_{pa}(T_{bj}, h_{bj}) \tag{6}$$

$$\left| H_c(T_c / T_{bj}, h_c) \right| = \sqrt{\frac{1 + 4(h_c / \gamma_c)^2 (T_c / T_{bj})^2}{\{1 - (T_c / T_{bj})^2\}^2 + 4(h_c / \gamma_c)^2 (T_c / T_{bj})^2}} \tag{7}$$

where $|H_c(T_c / T_{bj}, h_c)|$ = transfer function of the system having T_c and h_c against input with period T_{bj}. However, since the actual input is not steady-state motion, this will result in lower peak value at the resonance point. A correction coefficient γ_c is applied to account for this reduction in the response (see Section 3.3). Fig .4a shows $|H_c(T_c / T_{bj}, h_c)|$ and Fig. 4b shows $S_{pac,j}(T_c, h_c)$ of prediction formula 1 generated under the conditions of Taft EW, $T_{bj} = 0.5, 2, 5$s, $h_{bj} = h_c = 0.02$, and $\gamma_c = 1$.
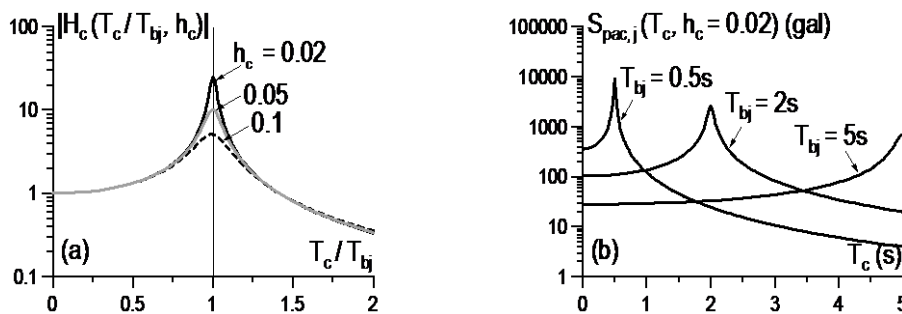

Fig. 4 – Prediction formula 1 and its transfer function (Taft EW, $h_{bj} = h_c = 0.02$, $\gamma_c = 1$)

3.2 Prediction formula 2 which considered tendancy of non-stationary response

Prediction formula 2 takes into account the influence of non-stationary response by recognizing the similarity between Fourier spectrum and undamped velocity spectrum for time history analysis in the frequency domain. The detailed derivation is described in Reference 13. Prediction formula 2 is expressed in Equation (8).

$$S_{pac,j}(T_c, h_c) = \left| H_b(T_{bj}/T_c, h_{bj}) \right| S_{pa}(T_c, h_c) \tag{8}$$

$$\left| H_b(T_{bj}/T_c, h_{bj}) \right| = \sqrt{\frac{1 + 4(h_{bj}/\gamma_{bj})^2 (T_{bj}/T_c)^2}{\{1 - (T_{bj}/T_c)^2\}^2 + 4(h_{bj}/\gamma_{bj})^2 (T_{bj}/T_c)^2}} \tag{9}$$

The expansion from undamped system ($h_{bj} \neq 0$ and $h_c \neq 0$) to damped system (h_{bj} and h_c) in Equation (8) causes an error in the vicinity of the resonance point. Therefore a correction coefficient γ_{bj} is introduced (section 3.3). Fig. 6a shows $|H_b(T_{bj}/T_c, h_{bj})|$, and Fig. 6b shows $S_{pac,j}(T_c, h_c)$ of prediction formula 2 as generated under the conditions of Taft EW, $T_{bj} = 0.5, 2, 5s$, $h_{bj} = h_c = 0.02$, and $\gamma_{bj} = 1$.
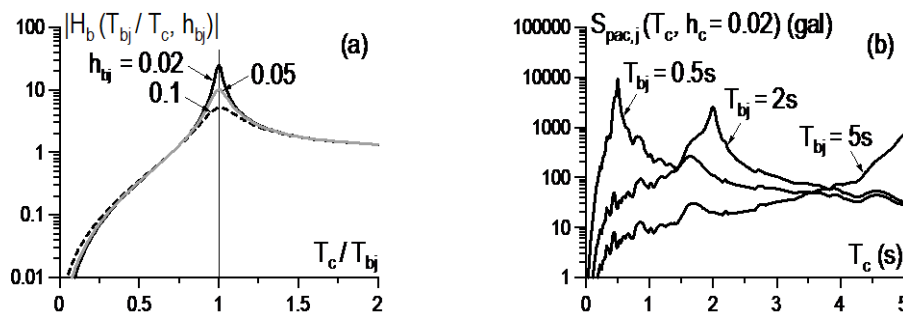

Fig. 6 – Prediction formula 2 and its transfer function (Taft EW, $h_{bj} = h_c = 0.02$, $\gamma_{bj} = 1$)

As shown in Fig. 6b, prediction formula 2 underestimates values in $T_c < T_{bj}$. Therefore, a correction term A_j is applied to Equation (8) to modify the response in the short-period range. The correction term A_j is determined based on time history analysis to correlate the prediction with the accurate solution in $T_c < T_{bj}$ and to take $S_{pa}(T_{bj}, h_{bj})$ at $T_c = 0$. That is, prediction formula 2 is rewritten as follows

$$S_{pac,j}(T_c, h_c) = \left| H_b(T_{bj}/T_c, h_{bj}) \right| S_{pa}(T_c, h_c) + A_j \tag{10}$$

$$A_j = S_{pa}(T_{bj}, h_{bj}) \cdot \min\{1, \ 5(1 - T_c/T_{bj})\} \qquad (0 < T_c/T_{bj} \leq 1) \tag{11a}$$

The characteristics of the building response can be defined as the building vibration equivalent cycle t_d/T_{bj}. In the case of $t_d/T_{bj} \leq 2$ when this value is extremely small, Equation (11b) is used instead of (11a).

$$A_j = S_{pa}(T_{bj}, h_{bj}) \cdot \max\{0, \ 1 - (5/3)(T_c/T_{bj})\} \tag{11b}$$

Fig. 7a shows the form of the correction term A_j, Fig. 7b, c shows the changes in the response spectra of prediction formula 2 before and after correction.
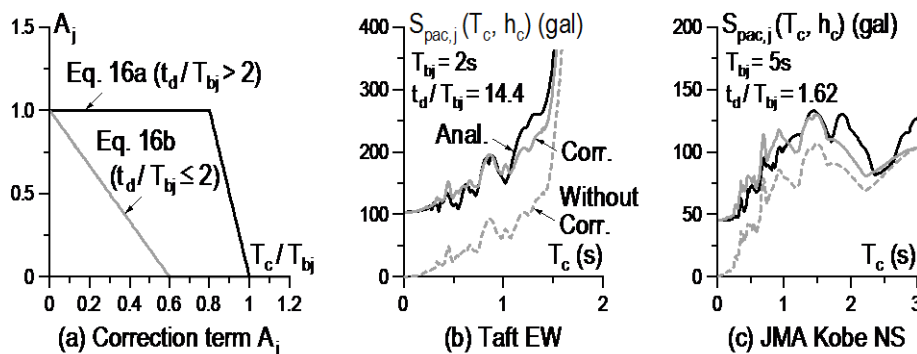

Fig. 7 – Changes due to correction term A_j ($h_{bj} = h_c = 0.02$)

6

3.3 Correction coefficients for resonance response

This section first presents the derivation of the correction coefficient γ_{bj} for prediction formula 2, and then the correction coefficient γ_c for prediction formula 1. The correction coefficient γ_{bj} is obtained as the value when the maximum acceleration ratio (the non-structural component and building) calculated by time history analysis to have the same value as the resonance amplification factor $\gamma_{bj} / 2h_{bj}$. Here $\gamma_{bj} / 2h_{bj}$ is obtained from substituting $T_{bj} / T_c = 1$ to $|H_b (T_{bj}/T_c, h_{bj})|$ (Eq. 9).

The relation of γ_{bj} and t_d / T_{bj} for 16 earthquake records with $T_{bj} = 0.5, 2, 5s$, $h_{bj} = 0.02, 0.1$, and $h_c = 0.02$, 0.1 is shown in Fig. 8. The correction coefficient γ_{bj} has a variation for each input seismic wave, where it increases linearly with increasing t_d/T_{bj} in the logarithmic axis except for the cases of Sylmar of which t_d / T_{bj} is extremely low. Furthermore, γ_{bj} also depends on damping ratios h_{bj} and h_c. It is higher for higher h_{bj} or smaller h_c. An approximate expression for γ_{bj} is presented in Equation (12) with a slope 0.05 and intercept $\xi_j (h_{bj}, h_c)$ as given by the solid line in Fig. 8.

$$\gamma_{bj} = (t_d / T_{bj})^{0.05} \cdot \xi_j(h_{bj}, h_c) \tag{12}$$
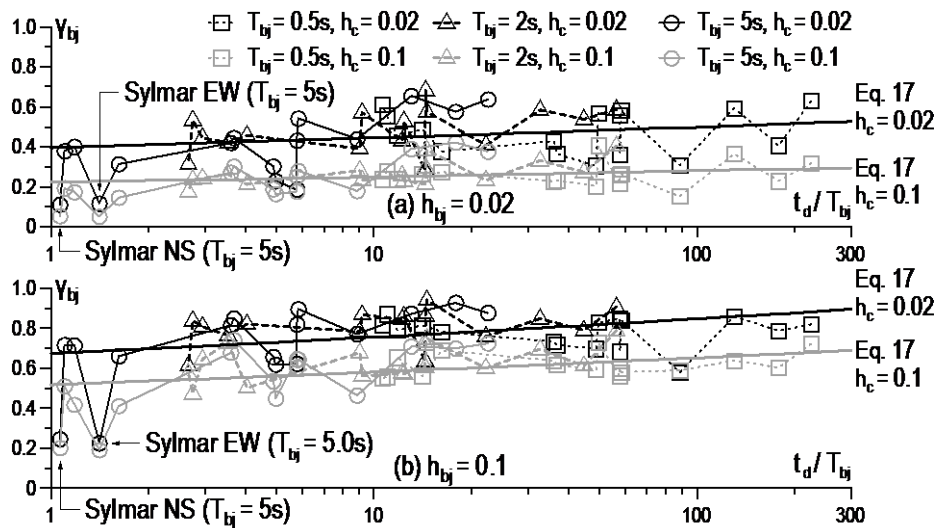

Fig. 8 – Correction coefficient γ_{bj} of prediction formula 2

The equation of $\xi_j(h_{bj}, h_c)$ in Equation (13) is derived as follows: (1) In the 100 combinations of $h_{bj} = 0.01$ to 0.1 and $h_c = 0.01$ to 0.1 (with increment of 0.01), 48 γ_{bj} are obtained from the combination cases of three natural periods $T_{bj} = T_c = 0.5, 2, 5s$ and 16 ground motions, (2) The average of 48 γ_{bj} is defined as $\xi_j^*(h_{bj}, h_c)$ at each h_{bj} and h_c value, (3) Apply the least squares approximation to $\xi_j^*(h_{bj}, h_c)$ to obtain the expression of $\xi_j(h_{bj}, h_c)$.

$$\xi_j(h_{bj}, h_c) = -48.7h_{bj}^2 + 23.4h_c^2 - 5.01h_{bj}h_c + 9.83h_{bj} - 4.61h_c + 0.28 \tag{13}$$

Fig. 9 presents the surfaces of $\xi_j^*(h_{bj}, h_c)$ and $\xi_j(h_{bj}, h_c)$ calculated by Equation (13). An applicable range of Equation (13) is $h_{bj} = 0.01$ to 0.1 and $h_c = 0.01$ to 0.1. Next, γ_c is determined from the values given by prediction formula 1 (Eq. 6) and 2 (Eq. 10) are equal at the resonance point ($T_c = T_{bj}, A_j = 0$)

$$\gamma_c = h_c B_j \sqrt{(\gamma_{bj} / h_{bj})^2 - (2 / B_j)^2 + 4}, \quad B_j = \frac{S_{pa}(T_c = T_{bj}, h_c)}{S_{pa}(T_{bj}, h_{bj})} \tag{14a, b}$$
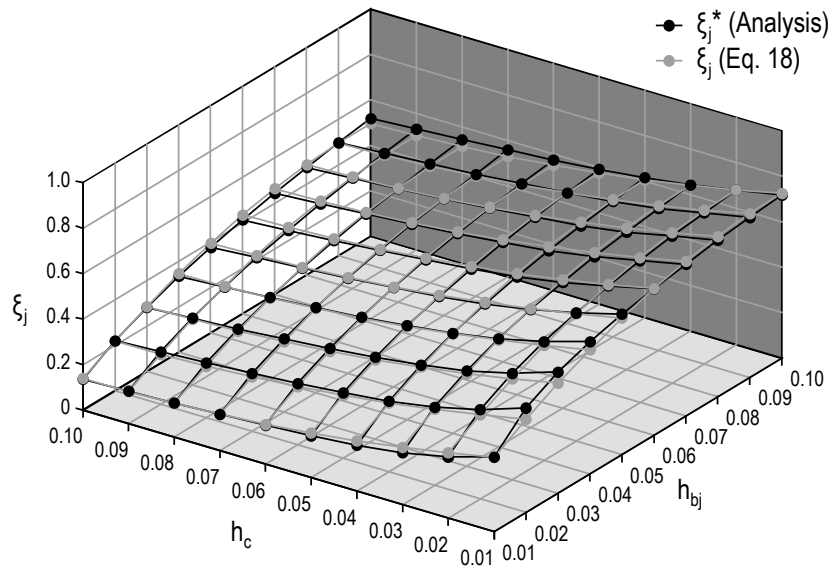
7

Fig. 9 – ξ_j in each damping ratio (mean of $\xi_j/\xi_j^* = 1.00$, standard deviation = 0.035)

The non-structural components have two typical response trends as mentioned above, although they are not differentiate clearly in the vicinity of $T_c = T_{bj}$. Hence, the larger value from prediction formula 1 or prediction formula 2 will take as the prediction value.

4. Verification for response prediction of non-structural components

Fig. 10 compares the prediction formula (Prediction) and the exact solution by detailed analysis of the non-structural pseudo-acceleration spectra $S_{pac,j}(T_c, h_c)$ for $T_c = 0.01$ to 5.00s (500 points, increment of 0.01s). The exact solution is obtained as $\omega_c^2|Y_j(t)|_{max}$ value from the time history solution $Y_j(t)$. Fig. 10a to c show the results obtained from three input seismic motions: (a) JMA Kobe NS ($t_d = 8.1$s) as pulse-like ground motion, (b) Hachinohe EW ($t_d = 24.8$s) as general ground motion, and (c) Tomakomai EW ($t_d = 89.5$s) as long-period ground motion. Four damping combinations (h_{bj}, h_c) = (0.02, 0.02), (0.02, 0.1), (0.1, 0.02), and (0.1, 0.1) are shown from upper row, and three spectral-curves for $T_{bj} = 0.5$, 2, and 5s are shown in each graph.

As shown in Fig. 10, the non-structural pseudo-acceleration spectral value is smaller when the natural period of the SDOF building model is longer. The accurate solution of $S_{pac,j}(T_c, h_c)$ has fluctuation which is attributed to the influence of ground motion characteristics. It is clearly observed the peak value of $S_{pac,j}(T_c, h_c)$ does not necessarily occur at the resonance point. The proposed prediction method can reproduce the spectral curves including uneven shapes with great accuracies.

Further, the prediction values of the resonance point ($T_c = T_{bj}$) by Kaneko's method are shown by the circle. Kaneko's method can accurately predict the resonance point as almost the same as the proposed method which demonstrates the accuracy of the proposed method. Fig. 11 shows the ratio obtained by dividing the predicted value by the acurate solution value to verify the accuracy and trend of the prediction formula. Its mean value and coefficient of variation for 500 points in the range of $T_c = 0.01$ to 5.00s are also shown. The accuracy of the prediction is very stable as demonstrated by the mean value of almost 1, the coefficient of variation less than 0.18, and the accuracy of the resonance point is comparable to the other points. However, for Hachinohe EW with $T_{bj} = 5$s, the correction by A_j of the prediction is on the safe side over a wide range (Fig. 11b). Fig. 12 compares the propsoed method with the BRI prediction method for the case of $h_{bj} = h_c = 0.05$. The BRI method cannot predict the fluctuations in the non-structural response spectrum due to the assumption of smooth curve, and noticeable error occurs in the range of $T_c > T_{bj}$.

8

The non-structural displacement spectra obtained from multiplying $S_{pac,j}(T_c, h_c)$ in Fig. 10 by $(T_c / 2\pi)^2$ for $h_{bj} = h_c = 0.02$ are shown in Fig. 13. In contrast to $S_{pac,j}(T_c, h_c)$, it is observed that the value increases depending on T_c. In particular for the long-period ground motion Tomakomai EW, the displacement response can be greater than the resonance point in the long period (Fig. 12c). The prediction method can reproduce this behavior trend with good accuray.
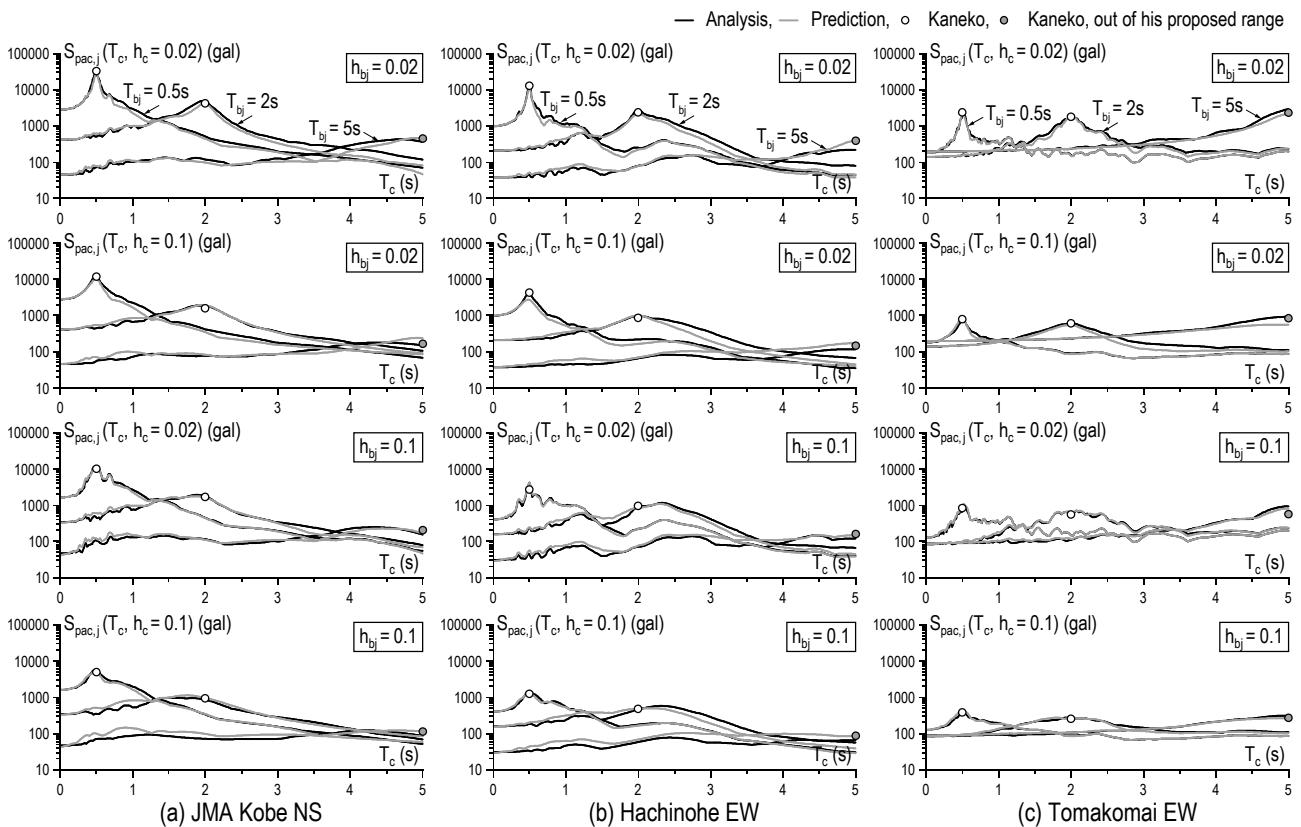
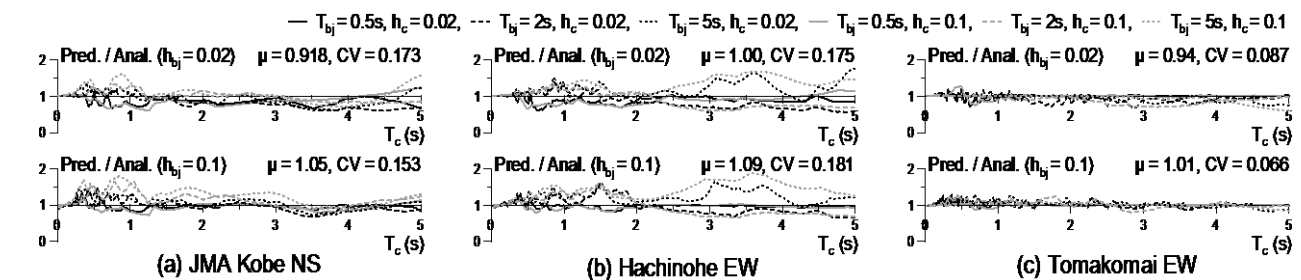Fig. 10 – Analysis vs. prediction: pseudo-acceleration spectra of components

Fig. 11 – Prediction accuracies, μ = mean value for T_c = 0.01 to 5s, σ = std. deviation, CV = σ / μ
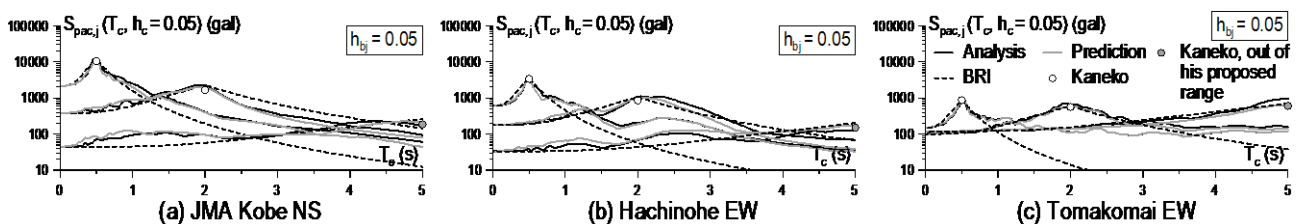

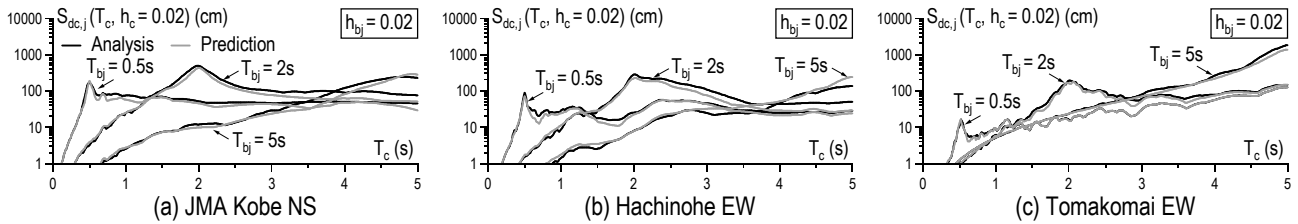Fig. 12 – Cpmparison with BRI method (available only for $h_{bj} = h_c = 0.05$)

9

Fig. 13 – Analysis vs. prediction: displacement spectra of components

As shown in Table 2a, the overall accuracy of the proposed method method is stable. The accuracy of the prediction at the resonance point is comparable to Kaneko's method (Table 2b). The error of the BRI method (Fig. 12) is noticeable for $T_{bj} = 0.5$s (Table 2c). Further, in the combination case of Sylmar ($t_d =$ 5.32s in NS, $t_d = 7.06$s in EW) and $T_{bj} = 5$s, with small t_d / T_{bj}, the peak response is shifted to shorter period side from the resonance point. This is attributed to the effect of pulse-like ground motion (see Appendix). This leads to overestimating the resonance point which is on the safe side. Table 2a to c also shows the statistics of 14 ground motions except Sylmar NS and EW for $T_{bj} = 5$s.

Table 2 – Prediction accuracies of SDOF models

Upper row: mean value for $T_c = 0.01$ to 5s (a and c), $T_c = T_{bj}$ (b), Lower row: std. deviation

(a) Proposed

Damping	$T_{bj} = 0.5$s 16 waves	$T_{bj} = 2$s 16 waves	$T_{bj} = 5$s 16 waves	$T_{bj} = 5$s Except Sylmar
$h_{bj} = 0.02$, $h_c = 0.02$	0.928 (0.074)	0.832 (0.163)	1.002 (0.235)	0.973 (0.157)
$h_{bj} = 0.02$, $h_c = 0.1$	0.907 (0.094)	0.886 (0.145)	1.076 (0.322)	1.028 (0.142)
$h_{bj} = 0.1$, $h_c = 0.02$	0.984 (0.057)	0.953 (0.153)	1.104 (0.220)	1.081 (0.152)
$h_{bj} = 0.1$, $h_c = 0.1$	0.965 (0.070)	0.958 (0.174)	1.169 (0.231)	1.139 (0.174)
All data	0.946 (0.074)	0.903 (0.162)	1.086 (0.257)	1.052 (0.156)

(b) Proposed vs. Kaneko for $T_c = T_{bj}$ only

Method	$T_{bj} = 0.5$s 16 waves	$T_{bj} = 2$s 16 waves	$T_{bj} = 5$s 16 waves	$T_{bj} = 5$s Except Sylmar
Proposed	1.052 (0.190)	0.960 (0.156)	1.324 (0.843)	1.028 (0.406)
Kaneko	1.066 (0.204)	0.956 (0.159)	1.280 (0.790)	1.000 (0.383)

Note:

"All Data" means 5 cases for $(h_{bj}, h_c) = (0.02, 0.02)$, $(0.02, 0.1)$, $(0.1, 0.02)$, $(0.1, 0.1)$, and $(0.05, 0.05)$
"Except Sylmar" shows 14-wave statistical values excepting Sylmar NS and EW for $T_{bj} = 5$s

(c) Proposed vs. BRI for $h_{bj} = h_c = 0.05$ only

Method	$T_{bj} = 0.5$s 16 waves	$T_{bj} = 2$s 16 waves	$T_{bj} = 5$s 16 waves	$T_{bj} = 5$s Except Sylmar
Proposed	0.947 (0.069)	0.886 (0.172)	1.076 (0.264)	1.039 (0.155)
BRI	0.376 (0.377)	1.095 (0.245)	1.014 (0.358)	0.986 (0.178)

10

5. Conclusion

An improved simplified generation method of the response spectra for the non-structural components attached to the building floor is proposed. The accuracy of the prediction using the propsed method for the maximum acceleration and displacement is demonstrated through comparison with the exact solutions based on time history analysis. Significant conclusions can be summarized as follows

1) When the building and non-structural components are both modeled as SDOF systems, the non-structural pseudo-acceleration and displacement response spectra can be generated by using two transfer functions which represent the effects of the steady-state motion with the building period and the seismic ground motion to the non-structural components, the building maximum acceleration, and the seismic response spectrum.

2) The proposed method is derived based on analysis using 16 earthquake records with different durations and spectral characteristics, and extensive variations of the period and damping ratio of the building and non-structural components. The method can predict the maximum acceleration of the non-structural components and the maximum displacement against the building floor with excellent accuracy.

6. References

[1] Building Performance Standardization Association (2012): Jishin higai wo humaeta hikouzouzai no kijun no seibi ni kansuru kentou, http://www.mlit.go.jp/common/000208403.pdf.

[2] National Institute for Land and Infrastructure Management, Building Research Institute (2013): Kentikubutsu ni okeru tenjou datsuraku taisaku ni kakawaru gijutsukijun no kaisetsu.

[3] Ishihara T, Sato K, Suzuki K, Nagano M (2017): Proposal of a Direct Estimation Method for Floor Response Spectrum in Non-linear Seismic Behavior, *AIJ Journal of Technology and Design*, **54** (23), 433-436.

[4] Yasui Y, Yoshihara J, Takeda T, Miyamoto A (1993): Direct generation method for floor response spectra, *Proceedings of the 12th International Conference SMiRT*, K13/4, 367-372.

[5] Sullivan TJ, Calvi PM, Nascimbene R (2013): Towards Improved Floor Spectra Estimates for Seismic Design, *Earthquakes and Structures*, **4** (1), 109-132.

[6] Jiang W, Li B, Xie W, Pamdey MD (2015): Generate floor response spectra: Part 1. Direct Spectra-to-Spectra Method, *Nuclear Engineering and Design*, **293**, 525-546.

[7] Kaneko K (2016): Direct Evaluation Method of Floor Response Spectra from Specified Ground Response Spectra Based on Spectrum Difference Rule, *AIJ Journal of Structural and Construction Engineering*, **729** (81), 1789-1797.

[8] Kaneko K (2018): Expected Values of Dynamic Amplification Ratio of Nonstructural Components in Resonance Considering Significant Duration of Strong Ground Motions, *AIJ Journal of Structural and Construction Engineering*, **746** (83), 555-563.

[9] Kasai K, Komatsu S, Lau D (2020): A Prediction method of non-structural response spectra, Part 2: Verification of components in multi-story building, *17WCEE*, Sendai, JAPAN.

[10] Trifunac MD, Brady AG (1975): A Study on the Duration of Strong Earthquake Ground Motion, *Bulletin of the Seismological Society of America*, **65** (3), 581-626.

[11] Osaki Y (1996): Vibration Theory for Architectural Structures, *Shokokusha Publishing Co., Ltd.*

[12] Chopra AK (2016): Dynamic of Structures: Theory and Applications to Earthquake Engineering.

[13] Kasai K, Komatsu S, Kondo S, Akatsuka N (2019): Seismic response spectrum rule for non-structural components in buildings, *AIJ Journal of Structural and Construction Engineering*, **758** (84), 489-499.

11

Appendix

Considering about the variations of γ_{bj} observed in Fig. 8. Osaki has pointed out the approximate relation of the undamped-velocity spectrum $S_{pv}(\omega, h_{bj} = 0)$ and Fourier spectrum $|F_{\ddot{u}_g}(\omega)|$, but this relation fails around $T = 5$s, Sylmar NS as shown in Fig. A-1. This is due to, the building maximum absolute acceleration response $\ddot{X}_j(t) + \ddot{u}_g(t)$ of the SDOF building model with $T_{bj} = 5$s subjected to Sylmar NS is strongly affected by the short-period pulse (Fig. A-2). Whereas, the non-structural absolute acceleration response $\ddot{Y}_j(t) + \ddot{X}_j(t) + \ddot{u}_g(t)$ ($T_c = 5$s, $h_c = 0.02$) is dominated at period 5s by the resonance, so that the effect of short-period pulse is reduced in the actual non-structural response (Fig. A-3). The prediction based on the building pseudo-velocity spectrum considering this effects gives 3.42 times the prediction value ($\gamma_{bj} = 0.389$) of the exact solution ($\gamma_{bj} = 0.109$) for Sylmar NS, $T_{bj} = 5$s (Fig. A-4).
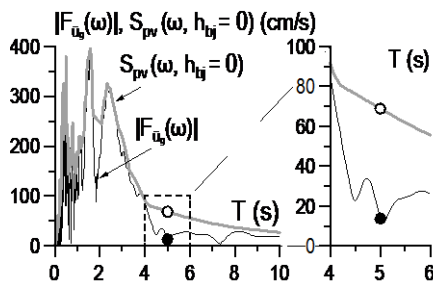

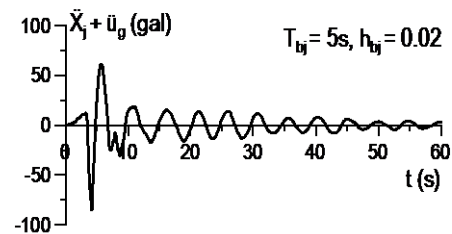Fig. A-1 – Fourier spectrum of ground motion and velocity spectrum of undamped building

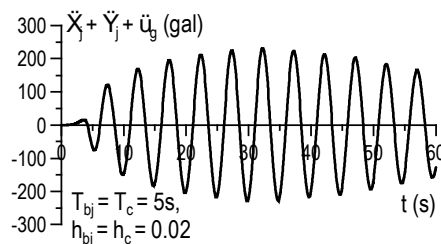Fig. A-2 – Absolute acceleration response of building

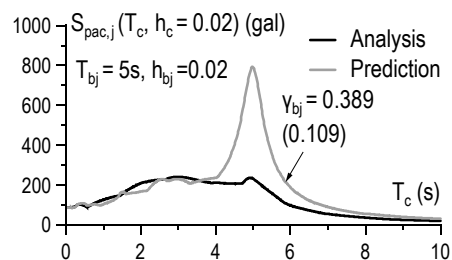Fig. A-3 – Absolute acceleration response of component

Fig. A-4 – Analysis vs. prediction: pseudo-acceleration spectrum of component

12